

NETWORK PERFORMANCE AND SEISMIC NOISE CHARACTERISATION IN THE WAIRAKEI GEOTHERMAL FIELD

C.M. Boese¹, J. Andrews¹ and F. Sepulveda²

¹Institute of Earth Science and Engineering, University of Auckland, 58 Symond Street, Auckland, New Zealand

²Contact Energy Limited, Wairakei Power Station, SH1, Taupo, New Zealand

c.boese@auckland.ac.nz

Keywords: *Seismic background noise, earthquake detection, borehole seismometers, magnitude of catalogue completeness*

ABSTRACT

Characterising microseismicity in developed geothermal fields can be useful for understanding deep reservoir structure and the response to field development and operations. The ability to detect microearthquakes of interest depends on the design of the network and prevailing background seismic noise levels. Developed geothermal fields can be affected by a range of anthropogenic noise sources, particularly those associated with geothermal power plant infrastructure (e.g. power house, steamfield, drilling, traffic, civil works etc.), as well as natural background noise sources (e.g. ocean and meteorological activity) including those specific to a geothermal environment (subsurface fluid movement). How extensively seismic monitoring instrumentation is deployed throughout the field is usually a trade-off between site availability, access, cost and desired monitoring objectives (coverage and detection). Incorporation of borehole seismometers can result in significant improvements in signal to noise ratios and greater number of detected microseismic events relative to surface seismic station networks. Subsequently, borehole networks have the potential to provide more useful information about the reservoir.

We investigate noise characteristics and array performance for a network of borehole seismometers deployed at the Wairakei geothermal field. An assessment is made of noise levels arising from various sources. Borehole sensors at different depth levels are compared to study the relative improvement in noise isolation with depth. Implications for magnitude and detection thresholds for station depths across the network are discussed. We review the network coverage and discuss general guidelines for planning seismic instrumentation of a geothermal field to mitigate the effect of high and varying noise.

1. INTRODUCTION

1.1 Wairakei geothermal field

The Wairakei geothermal field is one of 23 high-temperature geothermal systems in the Taupo Volcanic Zone (TVZ; Bibby et al., 1995), a back-arc rift resulting from subduction of the Pacific Plate beneath the Australian Plate throughout the North Island of New Zealand.

Power generation at the Wairakei field, located north of Lake Taupo, commenced in 1958 (e.g. Bixley et al., 2009) and the field currently has a total installed capacity of 375 MWe across four power stations: Te Mihi, Wairakei, Pohipi (exploiting the southwest steam zone) and the Wairakei Binary plant. Injection commenced in 1997 in the

Otupu area and was extended to the Karapiti South area in 2011.

The field has been the subject of extensive studies, with over 200 wells drilled and a number of geophysical surveys carried out including resistivity, magnetic, gravity and seismic (e.g. summary by Hunt et al., 2009; Sepulveda et al., 2012; Sepulveda et al., 2013). Previous passive seismic monitoring of the area comprises permanent GeoNet stations, plus a number of temporary, small-scale seismic networks have been deployed at Wairakei including the monitoring of injection tests in 1984 (Sherburn, 1984) and 1987 – 1989 (Sherburn et al., 1990).

The setting is expected to be challenging for seismic monitoring. The subsurface stratigraphy of the Wairakei field is dominated by alternating products of rhyolitic volcanism, such as lavas and ignimbrites, and volcanic-derived sediments (Bignal et al., 2010). These infill materials have been shown to resonate at certain frequencies (Bannister & Meluish, 1997; for the Kaingaroa plateau) and could potentially channel noise created by the geothermal operations in the Wairakei geothermal field.

1.2 Seismic Networks

1.2.1 GeoNet Surface Network

The GeoNet network is the most extensive seismic monitoring array in New Zealand with the longest-operating history (regional coverage since 1987), and has played a key role in improving our understanding of seismicity in the TVZ (e.g. Bryan et al., 1999). GeoNet operates two regional short-period seismometer networks in the central TVZ, the Rotorua-Tarawera and the Ruapehu-Tongariro networks (Fig.1). A total of 17 stations from these networks enclose the Wairakei geothermal field with an average station spacing of 13.9 km. Additional small, dense networks have also been deployed in the area but do not add significant additional coverage for our field.

1.2.2 Wairakei Borehole Station Network

In 2009 Contact Energy commenced seismic monitoring of the Wairakei geothermal field with a high-sensitivity borehole network. By March 2009 the first stage of installation had been completed with the deployment of nine borehole plus one surface seismometer. During 2012 and early 2013, an additional four borehole seismometers were added to expand coverage to the south, west and south-east (Sepulveda et al., 2013). Stations are permanently installed at depths ranging between 60 and 1200 m (Table 1) with an average station spacing of 2.6 km. The Wairakei Station Network (WSN) was complete in its current configuration by March 2013.

Table 1: Station information for the permanent borehole seismometers in the Wairakei Station Network (see also information provided by Sepulveda et al., 2013).

Station ID	Borehole ID	Sensor Depth (m)	Elev. (MSL) (m)
T01	THEQ01	80	337
T02	THEQ02	80	383
W01	WKM09	92	293
W02	WKEQ02	80	380
W03	WKEQ03	80	459
W04	WKEQ04	80	369
W05	WKEQ05	156	326
W06	WKEQ06	153	368
W07	WKEQ07	60	444
W08	WKEQ08	120	401
W09	WKEQ09	80	516
W10	WK402	1194	-760
W11	WK313	1209	-869
W19	WK227	300	97

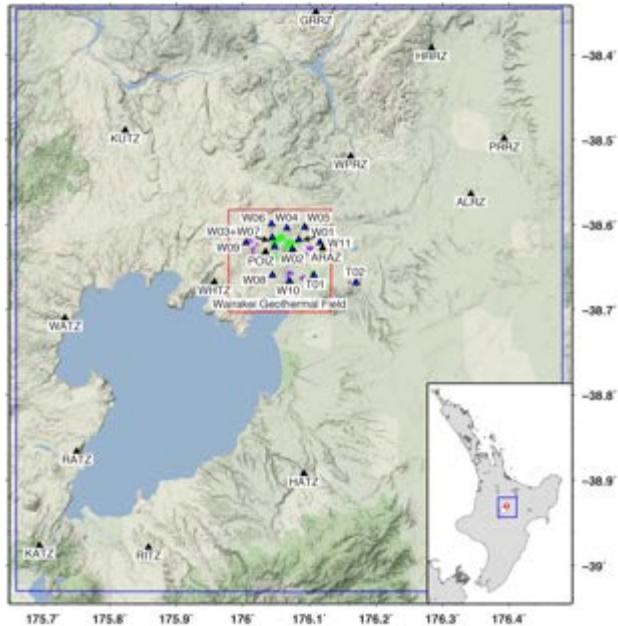


Figure 1: Overview of the Wairakei geothermal field in the central TVZ and the station networks in operation within (WSN) and surrounding the Wairakei geothermal field (GeoNet). The red square outlines the study area, the blue one the larger region surrounding the field. Production (green) and injection (purple) wells are marked.

2. METHODS

We have employed several analysis methods to explore network performance (magnitude of catalogue completeness of the seismic networks, magnitude detection thresholds of individual stations) and to investigate background noise (time and frequency characteristics, identification of dominant noise sources).

Magnitudes calculated for the Wairakei earthquake catalogue are moment magnitudes which are based on the seismic moment M_0 , a static measure that incorporates the area of fault rupture, the average amount of slip, and the force that was required to overcome the friction of the rocks that were offset by faulting.

The seismic moment is derived using the method described by Andrews (1986),

$$M_0 = 4\pi\rho\beta^3 \frac{\Omega}{R}$$

where ρ is the density (g/cm^3), β the shear-wave velocity (cm/s), Ω the low-frequency spectral level (cm^2/s), and R a correction factor for the radiation pattern of the S-wave. Appropriate values for the field are chosen for the density and shear-wave velocity. The moment determination is automated and run on unfiltered waveforms.

The moment magnitude is calculated following the formula given by Hanks & Kanamori (1979)

$$M_w = \frac{\log M_0}{a} - b$$

in which M_w indicates moment magnitude, and M_0 represents the seismic moment ($\text{dyn}\cdot\text{cm}$). The constants in this formula, representing slope and M_w -axis intercept are specific to local geology and require regional calibration from the standard values of $a = 1.5$ and $b = 10.73$. For the Wairakei geothermal field, these constants were found to be $a = 0.9825$ and $b = 17.61$ based on initial magnitude calibration on the local magnitudes derived by GeoNet. With the acquisition of more data in recent years by both WSN and GeoNet networks, an opportunity is available for a revised WSN magnitude calibration against moment magnitudes determined by GeoNet from regional moment tensor inversion (goes beyond the scope of this study).

The ability of a seismic network to detect earthquakes is given by the minimum magnitude of detection and the magnitude of catalogue completeness. We determine the magnitude of completeness and the b-value simultaneously using Aki's maximum likelihood method (Aki, 1965):

$$b = \frac{\log e}{M_A - M_C}$$

Where M_A is the average magnitude of earthquakes with $M \geq M_C$ and M_C is the magnitude cut-off. The b-value is visually picked from the plateau corresponding to the stable range of M_C (following Jacobs et al. 2013).

In order to compare the relative performance of the stations of the WSN, we calculate the average daily noise based on noise classification procedures proposed by Groos & Ritter (2009) to look at long-term temporal changes in the background noise.

To assess the noise per frequency band at each station we calculate the power spectral densities using the PASSCAL Quick Look eXtended (PQLX) tool (McNamara & Buland, 2004; McNamara & Boaz, 2006, 2011). After removing the instrument response, the mean and the trend of the data, the PQLX algorithm calculates the square of the acceleration amplitude spectra using the fast Fourier transform method on 60 min-long tapered records with 50% overlap. The

probability density function is computed for all power spectral densities to determine the median and standard deviation of the background noise at each site (McNamara & Buland, 2004).

Significant temporal changes in the noise level were investigated by plotting the particle motion of the noise in a narrow frequency band around the noise to identify any directionality that points back to the noise source.

The general performance of individual stations can be graphically assessed by simultaneously plotting picked and unpicked events against distance for all located earthquakes in the catalogue. In interpreting these plots (see Figure 5 for further explanation), station-event distribution must be taken into account. For instance, low magnitude events can be detected within a few kilometers distance of a station but this minimum magnitude of detectable events increases with distance due to geometrical spreading and attenuation of seismic energy. Therefore the percentage of picked events versus distance reflects at what distance from the station the event detection becomes affected by local noise levels and the depth of deployment.

Individual detection distances for each station are used in a simple grid search to calculate the volume illuminated by at least four stations, thus the assumed region where reliable locations can be obtained for nominal magnitude ranges 0 to 0.4 and -0.4 to 0 when all stations are operational. The illuminated volume can be expected to be increased with the use of additional stations or deployments of seismic sensors at greater depth.

3. RESULTS

3.0 Magnitude of catalogue completeness

We determine the magnitude of catalogue completeness – also termed cut-off magnitude – for the GeoNet and the WSN catalogues for the area comprising the Wairakei geothermal field (as shown in red in Figure 1) in different time periods.

Results for M_C and b-value found by application of Aki's maximum likelihood method to WSN and GeoNet catalogues in different time periods are summarized in Table 2 and results for current operation periods are shown in Figure 2. Both networks show the impact of increased station numbers leading to a decrease in magnitude of completeness: a drop from 2.2 to 1.75 for GeoNet is seen after 2007; a decrease from 1.1 to 0.2 for WSN after 2012. The installation of a second deep station in the network is thought to have a strong influence in the latter case.

Table 2: Results for M_C and b-value from application of Aki's maximum likelihood method to WSN and GeoNet catalogues in different time periods.

Network	Date Range	Number of events	M_C	b-value
GeoNet	1.1.1997 – 1.1.2007	326	2.2	1.20
GeoNet	1.1.2008 – 1.1.2012	203	1.75	1.20
WSN	1.1.2009 – 1.1.2013	3086	1.1	0.95
WSN	1.1.2013 – 1.7.2014	4329	0.2	0.95

The purpose of the WSN was to achieve monitoring in the noisy study area and this dense, borehole network therefore has a significantly smaller magnitude of completeness compared to the GeoNet network. Based on the Gutenberg-Richter relationship (Gutenberg and Richter, 1944) the expected number of earthquakes of low relative to high magnitudes increases tenfold with every decrease of one magnitude unit given a b-value of 1. The implication is that for every 100 events of $M >= 1.7$ recorded by GeoNet, approximately 3160 events of $M >= 0.2$ are expected to be recorded by WSN.

The b-value of 1.2 obtained in the Wairakei area using the GeoNet data (2008-2012) would suggest higher numbers of small earthquakes in the Wairakei geothermal field than actually recorded by the local WSN (b-value 0.95 during 2012-2013). In this case, the b-value derived from the GeoNet catalogue is most likely over-estimated due to unrepresentative sampling of the seismicity over a recording period that is too short for the seismicity range considered (1.75 to 3.2).

An accurate b-value estimate is important because it has been hypothesized that different physical triggers (e.g. stress-induced tectonic event, fluid-assisted faulting, volcanic tremor etc.) can result in different b-values, which can be potentially useful in the interpretation of causative mechanisms (e.g. natural versus induced seismicity). A comprehensive interpretation of b-values in terms of physical triggers requires a detailed study of variations in time and space, which is beyond the scope of this study. Here, the comparison of b-values is used mainly to assess the completeness of the seismic record.

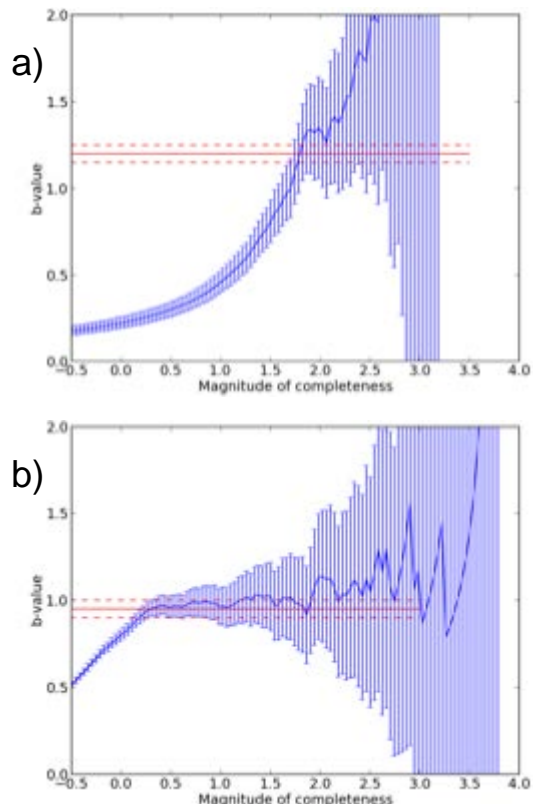


Figure 2: a) Magnitude of catalogue completeness ($M_C=1.75$) and b-value for the GeoNet network for the time period 1.1.2008 to 1.1.2012 based on 203 events and b) Magnitude of catalogue completeness ($M_C=0.2$) and b-value for the WSN network for the time period 1.1.2013 to 1.7.2014 based on 4329 events.

b) for the WSN ($M_C=0.2$) for the period 1.1.2013 and 31.5.2014 from 4329 events.

3.1 Earthquake detection

The magnitude of catalogue completeness and the minimum magnitude of detection are dependent on the station spacing and proximity to the earthquakes. Figure 3 shows the magnitudes of earthquakes in the Wairakei field from the GeoNet catalogue between 1995 and 2014 (with a gap between March 2012 and April 2013) together with the number of GeoNet stations (blue) recording in the area surrounding the Wairakei geothermal field. The minimum magnitude event detected in the GeoNet catalogue for the full period is 0.52.

Some variation in the magnitude of the detected earthquakes with time is seen in Figure 3 due to the number of operational stations and the background noise level. Once the Wairakei borehole station network (WSN, red) became operational by early 2009, the magnitude of catalogue completeness dropped significantly and again once the WSN was completed in early 2013 when the last stations were installed. The minimum magnitude event detected in the WSN catalogue during its operation is -0.91

The WSN is able to detect actual event numbers of microearthquakes for $M>=0.2$ where as the GeoNet network can only give approximate numbers of theoretically expected events. Using the observation by GeoNet of 25 events per year above magnitude 1.8 (average for four years 2008 – 2012), a b-value of 1.2 (Table 2) would predict approximately 2000 events above magnitude 0.2. However, the WSN observed only 1400 - 1500 events (2013 – 2014; only full year of recording with M_C of 0.2).

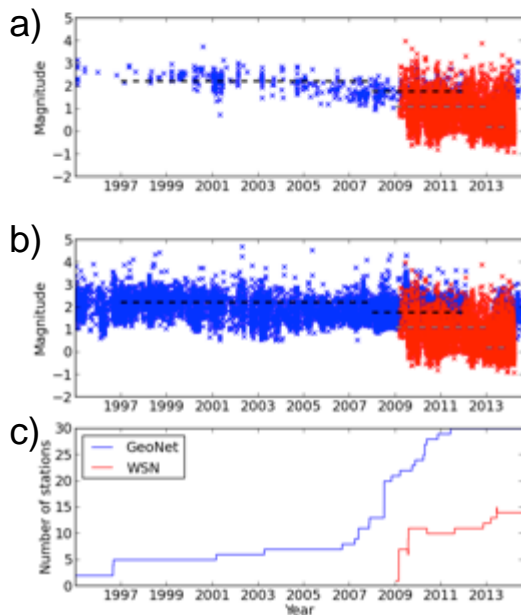


Figure 3: Comparison of magnitude of the earthquakes with time recorded in a) the Wairakei geothermal field and b) within the region surrounding the Wairakei geothermal field (areas as shown in Figure 1) by GeoNet (blue) and WSN (red). Black (GeoNet) and grey (WSN) dashed lines mark the magnitude of catalogue

completeness for the time period specified. c) The number of stations operating and the changes to the surface and borehole networks with time.

3.2 Depth improvement

Anthropogenic and natural noise rapidly decreases with depth. To illustrate this, we compare the surface sensor at site W07 with the best station (W04) installed at 60–92 m depth, the best station (W06) at 120–156 m depth, a 300 m deep temporary station (W19), and the best station at ca. 1200 m depth (W11) in Figure 4a.

A general decrease in the median noise with depth is seen at frequencies between 1 Hz and 20 Hz (periods 0.05 to 1 s), the main frequency range for surface noise sources such as roads, machinery, rivers etc. (1 – 25 Hz; Groos & Ritter, 2009). W19 is an outlier in that it shows higher noise levels in this frequency band despite the greater installation depth than W04 and W06. This could be due to above average local noise or be related to the temporary installation of this site.

Above 20 Hz the depth effect is not as evident, and at these frequencies other sources such as electrical noise are important. W19 and W11, which are spatially close, show elevated noise in a narrow band at high frequencies (20 to 40 Hz) potentially resulting from anthropogenic activity nearby.

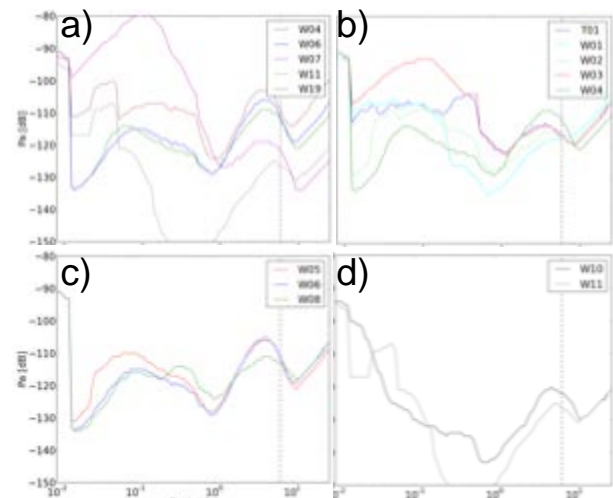


Figure 4: Median noise levels on the first horizontal channel (except for W19 for which the second horizontal channel was used) in comparison for a) different depth levels, and for stations at the same depth level of b) 60–92 m, c) 120–156 m and d) approx. 1200 m depth. The grey dashed line marks the approximate limit of sensor sensitivity.

3.2 Variability throughout the borehole network

Lateral variation in noise for sensors at the same depth level are illustrated in Figure 4 (b-d). Large differences (of ca. 20 dB) are seen in the high frequency/short period range for the 60–92 m deep stations, suggesting they are still significantly affected by surface noise. Noise differences for the stations at 120–156 m depth and the deepest stations (1194 and 1209 m depth) are less pronounced and restricted to narrower frequency bands.

3.3 Station detection ranges

A station will record all earthquakes of certain magnitude within its detection range and only those events above the cut-off magnitude within the whole study area. Figure 5 illustrates the station performance in the form of the detection percentage for earthquakes in the moment magnitude range 0 to 0.4, and 0.5 km distance bins from the station, reflecting the detection capabilities of selected stations within the Wairakei geothermal field. Stations were selected to show the variation across the field.

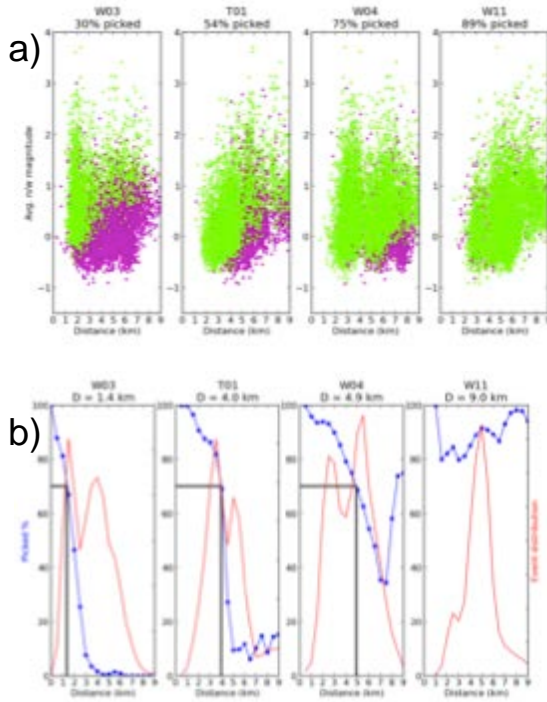


Figure 5: a) plots showing picked (green) and unpicked (magenta) events for four stations in the WSN plotted as magnitude against distance; b) plots showing detection percentage (blue) against distance for events in the magnitude range 0 – 0.4 for four stations in the WSN. The distance distribution of all events in the magnitude range 0 – 0.4 relative to the station is shown in red.

Station W03, which is sited most closely to power station operations, records approximately one third of the total number of located events due to high background noise levels. Stations T01 and W04 show increasing detection ranges due to reduced background noise. The deepest borehole station W11 shows the highest detection rates as would be expected from the very low noise levels.

3.3 Long-term temporal noise variation throughout the Wairakei geothermal field

The average daily noise level in the frequency range 1–25 Hz is plotted for three selected stations in Figure 6. These examples illustrate pronounced temporal noise changes with weekly patterns, working week versus holiday (e.g. Christmas break) patterns, and temporal anthropogenic activity near the site.

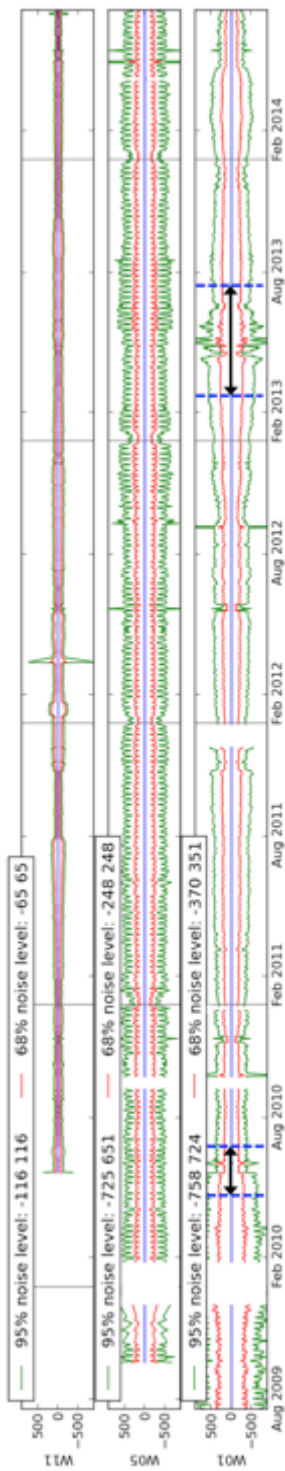


Figure 6: Minimum daily noise levels on the horizontal components of three selected stations of the WSN in the frequency band 1–25 Hz for the recording period end 2009–mid 2014. Station W11 is the deepest borehole station (1200 m) and is shown in comparison to a station at intermediate depths (W05, 156 m) and a shallow one (W01, 80 m). Christmas day each year is marked with a grey line. Periods of noticeable change in noise level at station W01 are shown by blue dashed lines and arrows.

The temporal character of noise experienced by each station in the WSN is summarised in Table 3. This distinguishes between daily, weekly and long-term variations. A depth effect is evident, for example stations W10 and W11 show little daily and no weekly noise variations, confirming their good isolation from surface anthropogenic noise sources. The stations with pronounced long-term variations in noise level are spatially correlated with geothermal power production infrastructure. Stations showing weekly noise are those that are close to anthropogenic noise sources (roads, construction etc.) but are largely unaffected by geothermal power operations.

Table 3: Summary of noise experienced by stations in the WSN, categorized as daily, weekly or longer-term variations. Noise not observed is marked red, noise observed is marked green and if some noise in a category is observed but is not strong it is marked yellow.

	W01	W02	W03	W04	W05	W06	W07	W08	W09	W10	W11	T01	T02
Daily	Yellow	Green	Green	Yellow	Yellow	Green	Green						
Weekly	Red	Red	Red	Green	Green	Green	Red	Yellow	Red	Red	Red	Yellow	Yellow
Long	Green	Green	Green	Red	Red	Red	Green	Yellow	Red	Red	Green	Yellow	Red

Due to temporally varying noise sources, station performance can differ over short and long time periods. Figure 7 shows two examples of obvious changes of anthropogenic noise sources at certain frequencies during the given recording period. At station W03, operations near the station changed resulting in a decrease in amplitude of noise at 40 Hz. At T01, interruption of nearby operations, presumably machinery, results in a noise change at frequencies of 35 and 70 Hz. For those and other similar cases aerial photos were checked for identifiable noise sources nearby and in most cases power infrastructure was found nearby. If the noise is organized, the particle motion of the noise often points towards the source, and can therefore help with identification. Once the source has been found, measures can be taken to reduce the impact on the nearby stations (e.g. by reducing coupling of the noise source into the ground).

4. DISCUSSION

The cut-off magnitude of 0.2 obtained from the WSN earthquake catalogue is significantly lower than that obtained for the GeoNet data due to smaller station spacing and borehole deployments. This has allowed a more accurate characterisation of the b-value for the recent monitoring period. Due to low numbers of larger magnitude events ($M>=2$) within the field itself, very long time periods are needed to accurately determine the b-value from less sensitive network catalogues. Both M_c and b-value are shown to vary with number of stations in the array, for both GeoNet and WSN. It has been shown that significant numbers of events are needed to achieve high-accuracy estimates of the b-value. Schorlemmer et al., (2005) consider estimates based on fewer than 200 events as marginal. An accurate b-value allows better characterization of the seismicity (and by implication stress), its temporal and spatial evolution, and allows more reliable and effective modelling and forecasting of seismicity throughout the field.

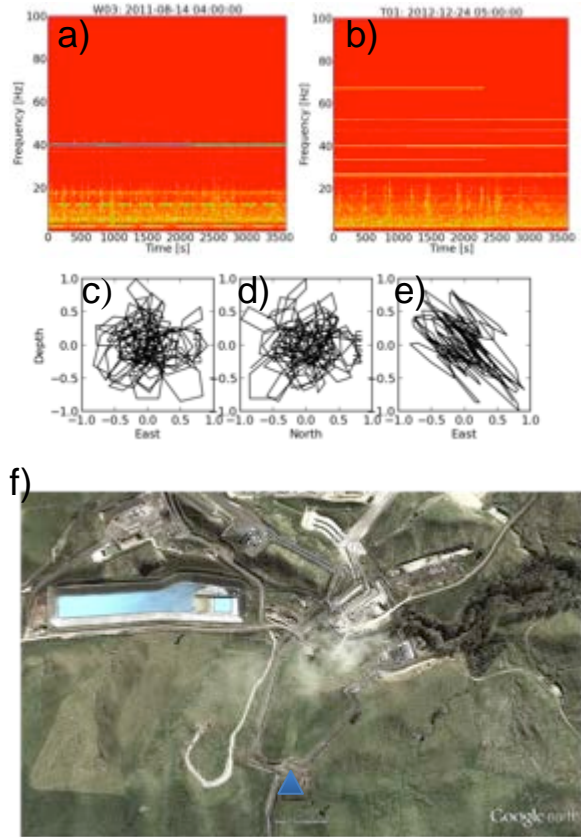


Figure 7: Spectrogram at stations a) W03 and b) T01 showing changes in the noise at certain frequencies typical for anthropogenic operations. The particle motion of the noise shows randomness in the c) Up-Down/East-West and d) Up-Down/North-South planes but strong directionality in the e) horizontal plane for the frequency range 35–42 Hz at W03. f) This may correspond to operations at the Te Mihi power plant nearby.

Elevated b-values (higher than 1) have been seen in environments analogous to our field site, both natural (volcanic settings) and artificial (hydrofracking sites and some other geothermal sites; Soultz, Dorbath et al. 2009; Coso, Kaven et al., 2013). It has also generally been thought that fluid injections lead to high b-values, however some geothermal areas and injection sites (Cooper Basin, Baisch et al., 2006; Preese Hall) have noted lower b-values. The obtained b-value result of 0.95 from the WSN is consistent with the global average in normal faulting regimes of 1 (Schorlemmer et al., 2005 and references therein) and therefore would be consistent with the extensional environment of the TVZ and may suggest that the stress state in the reservoir is not significantly or widespread disturbed. However, our value is slightly higher than previously derived values for the Wairakei area of 0.6 by Sherburn (1984) and 0.7 \pm 0.2 by Hunt & Latter (1982). Without further additional work to calibrate the WSN magnitude scale with GeoNet and to investigate the surrounding area, it is not possible to use our b-value for further interpretation.

Isolation from anthropogenic and natural noise sources increases with the sensor's deployment depth as seen for the WSN. However, at 60 m depth the noise experienced by our stations is still strongly dependent on varying surface

noise levels. Relatively good isolation from most common noise sources such as traffic and machinery is achieved in the depth range between 60 and 150 m. However, local geology is an important factor, especially when layers can form noise traps at depth and this should also be considered during site selection. Deep deployments (> 1 km) show the largest noise level improvement in the frequency range 1–25 Hz similar to that seen by Boese et al. 2014 for multiple level borehole stations in Auckland.

Miller et al. (2014) showed that the TVZ is a high noise environment in the frequency band 5–10 Hz compared to other regions in the North Island (their Fig. 7). The noise levels are 55 dB above the global reference (New Low Noise Model by Peterson et al. 1993) at 5–10 Hz in the area of the Wairakei Geothermal field, which poses a challenge for microearthquake monitoring. Noise sources in the Wairakei field are found to be highly variable. Stations with highest noise show no anthropogenic (weekly/daily) variability and a strong directionality in the particle motion of the noise, most likely related to adjacent power generation infrastructure. Locating stations at a distance from the anthropogenic noise sources (> 0.5 km) is critical to optimising station performance and detection ranges. Weekly noise variation is only seen at stations in sufficiently quiet noise environments, which is the achieved at all the stations in the 120–156 m depth range and for W04 at 80 m depth.

The magnitude–distance observations obtained in Figure 5 can be used to derive a detection distance for each station using a percentage success threshold ($\geq 70\%$). In the case where more than 70% of events were detected over the full distance range considered, a user-set value equal to the approximate array aperture (9 km) was used. Using the so-determined detection ranges of each station in the WSN, the coverage of the Wairakei geothermal field for events in the magnitude ranges 0–0.4 and -0.4–0 is shown in Figure 8. The central Wairakei field is adequately covered for microearthquakes with magnitudes $M \geq -0.4$. However, coverage of the boundaries of the field decreases rapidly with decreasing magnitude, especially at sites associated with out-of-field geothermal operations. The integration of data from two private GeoNet stations POIZ and ARAZ would potentially contribute to improving the coverage, however, both stations exhibit high noise in the frequency range of interest (both show levels significantly above the New High Noise Model reference level).

The coverage in two important parts of the field with out-of-field operations – Poihipi and Karapiti to Tauhara – could be significantly extended by adding two new borehole stations as shown in Figure 9. If we assume that the detection ranges of these two stations would be comparable to other sites within the WSN, this would link the detection ranges of stations T02 and W09 to those of the remaining stations and increase the coverage substantially.

5. CONCLUSION

The WSN provides high sensitivity microseismic monitoring of the Wairakei geothermal field with a magnitude of completeness 0.2. This allows detection of increased number of seismic events relative to regional networks and accurate characterisation of the b-value (0.95), a critical parameter for modelling and forecasting.

At Wairakei, deployment of seismometers at depths greater than 100 m was observed to best isolate sensors from most

surface noise, though location at least 0.5 km from significant sources such as geothermal power generation operations is necessary to optimise station performance.

The WSN has good coverage down to magnitude -0.4 for main geothermal and injection sites. The various techniques discussed here can feed into field planning and monitoring in terms of optimal location of additional seismic stations for increased sensitivity in peripheral operational areas.

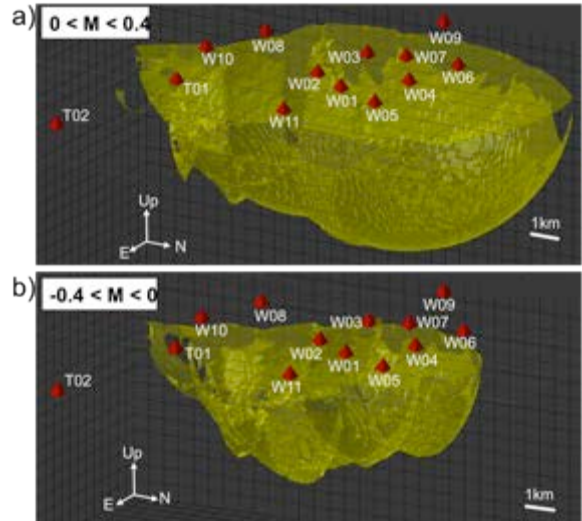


Figure 8: Coverage of the Wairakei geothermal field using the 70%-detection magnitude versus distance information for individual stations of the WSN.

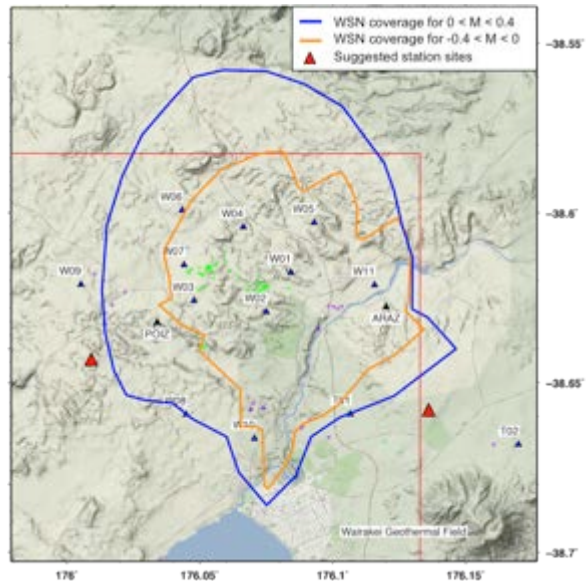


Figure 9: Lateral coverage (at shallow depths) of the Wairakei geothermal field by the WSN using the 70%-detection distance for two magnitude ranges (blue: 0 – 0.4; orange: -0.4 – 0). Production (green) and injection (purple) wells are marked. To achieve the same coverage at Poihipi (near W09) and Karapiti (near W10) injection and Tauhara production (SE of T01) sites, two new station locations are suggested.

ACKNOWLEDGEMENTS

The authors would like to thank Contact Energy Ltd. for their ongoing support and permission to publish data. We

would also like to acknowledge GeoNet and its sponsors, the EQC, GNS Science and LINZ.

REFERENCES

Aki, K.: Maximum likelihood estimate of b in the formula $\log N = a - bM$ and its confidence limits. *Bull. Earthq. Res. Inst. Univ. Tokyo*, **43**, 237-239, (1965).

Andrews, D.J.: Objective determination of source parameters and similarity of earthquakes of different size. *Earthquake source mechanics*, 259-267, (1986).

Baisch, S., Vörös, R., Weidler, R. and Wyborn, D.: Investigation of fault mechanisms during geothermal reservoir stimulation experiments in the Cooper Basin, Australia. *Bull. Seis. Soc. Am.*, **99**(1), 148-158, (2009).

Bannister, S., and Melhuish, A.: Seismic scattering and reverberation, Kaingaroa plateau, Taupo Volcanic Zone, New Zealand. *New Zealand Journal of Geology and Geophysics*, **40** (3), 375-381, (1997).

Bibby, H.M., Caldwell, T.G., Davey, F.J. and Webb, T.H.: Geophysical evidence on the structure of the Taupo Volcanic Zone and its hydrothermal circulation. *J. Volcan. Geotherm. Res.*, **68**, 29-58, (1995).

Bixley, P.B., Clotworthy, A.W. and Mannington, W.I.: Evolution of the Wairakei geothermal reservoir during 50 years of production. *Geothermics*, **38**, 145-154, (2009).

Bignall, G., Milicich, S., Ramirez, E., Rosenberg, M., Kilgour, G. and Rae, A.: Geology of the Wairakei-Tauhara Geothermal System, New Zealand. *Proceedings World Geothermal Congress 2010*, Bali, Indonesia, 25-29 April, (2010).

Boese, C., Wotherspoon, L., Alvarez, M., and Malin, P.: Analysis of anthropogenic and natural noise from multi-level borehole seismometers in an urban environment, Auckland, New Zealand. *Bull. Seism. Soc. Am.* (in review).

Bryan, C.J., Sherburn, S., Bibby, H.M., Bannister, S.C. and Hurst, A.W.: Shallow seismicity of the central Taupo Volcanic Zone, New Zealand: its distribution and nature. *New Zealand Journal of Geology & Geophysics*, **42**, 533-542, (1999).

Dorbath, L., Cuenot, N., Genter, A. and Frogneux, M.: Seismic response of the fractured and faulted granite of Soultz-sous-Forêts (France) to 5 km deep massive water injections. *Geophys. J. Int.*, **177**, 653-675, (2009).

Groos, J.C., and Ritter, J.R.R.: Time domain classification and quantification of seismic noise in an urban environment. *Geophys. J. Int.*, **179**, 1213-1231, (2009).

Gutenberg, B., and Richter, C.F.: Frequency of earthquakes in California. *Bull. Seismol. Soc. Am.*, **34**, 185-188, (1944).

Hanks, T.C., Kanamori, H.: A moment magnitude scale. *J. Geophys. Res.: Solid Earth*, **84** (B5), 2348-2350, (1979).

Hunt, T.M., Latter, J.H.: A survey of seismic activity near Wairakei geothermal field, New Zealand. *J. Volcan. Geotherm. Res.*, **14**, 319-334, (1982).

Hunt, T.M., Bromley, C.J., Risk, G.F., Sherburn, S., Soengkono, S.: Geophysical investigations of the Wairakei field, *Geothermics*, **38**, 85-97, (2009).

Jacobs, K.M., Smith, E.G.C., Savage, M.K. and Zhuang, J.: Cumulative rate analysis (CURATE): A clustering algorithm for swarm dominated catalogs. *J. Geophys. Res.: Solid Earth*, **118**, 553-569, (2013).

Kaven, J.O., S.H. Hickman and Davatz, N.C.: Microseismicity within the Coso geothermal field, California, from 1996-2012. *Proceedings 38th Workshop on Geothermal Reservoir Engineering*, Stanford University, Stanford, California, February 11-13, (2013).

McNamara, D.E., and Buland R.P.: Ambient noise levels in the continental United States. *Bull. Seism. Soc. Am.*, **94** (4), 1517-1527, (2004).

McNamara, D.E., and Boaz R.: Seismic noise analysis system using power spectral density probability density functions: a stand-alone software package, USGS, (2006).

McNamara, D.E., and Boaz R.: PQLX: A seismic data quality control system description, applications and user's manual: U.S. Geological Survey Open-File Report 2010-1292, (2011).

Miller, C. A., and Jolly, A. D.: A model for developing best practice volcano monitoring: a combined threat assessment, consultation and network effectiveness approach. *Natural Hazards*, **71** (1), 493-522, (2014).

Peterson, J. (1993). Observations and modeling of seismic background noise. *U.S. Geological Survey Open-File Report 93-322*, (1993).

Schorlemmer, D., Wiemer, S., and Wyss, M.: Variations in earthquake-size distribution across different stress regimes. *Nature*, **437**(7058), 539-542, (2005).

Sepulveda, F., Mannington, W., Charroy, J., Soengkono, S. and Ussher, G.: Integrated approach to interpretation of magnetotelluric study at Wairakei, New Zealand. *Proceedings, Stanford Geothermal Workshop*, Stanford, CA, USA, (2012).

Sepulveda, F., Andrews, J., Alvarez, M., Montague, T. and Mannington, W.: Overview of deep structure using microseismicity at Wairakei. *Proceedings 6th New Zealand Geothermal Workshop*, 17-20 November, Rotorua, NZ, (2013).

Sherburn, S.: Seismic monitoring during a cold water injection experiment, Wairakei geothermal field: preliminary results. *Proceedings 35th New Zealand Geothermal Workshop*, (1984).

Sherburn, S., Allis, R. and Clotworthy, A.: Microseismic activity at Wairakei and Ohaaki geothermal fields. *Proceedings 12th New Zealand Geothermal Workshop*, (1990).